Macromolecules

pubs.acs.org/Macromolecules Article

Two-Dimensional Tetrathienonaphthalenes-Based Donor–Acceptor Copolymers: Synthesis, Isomeric Effect, and Organic Field-Effect Transistors

Huai-Hsuan Liu, Shao-Ling Chang, Kuo-Hsiu Huang, Fong-Yi Cao, Kuang-Yi Cheng, Han-Sheng Sun, Yu-Ying Lai, and Yen-Ju Cheng*

Cite This: *Macromolecules* 2020, 53, 7740–7748 Read Online

ACCESS | Metrics & More | Article Recommendations | Supporting Information

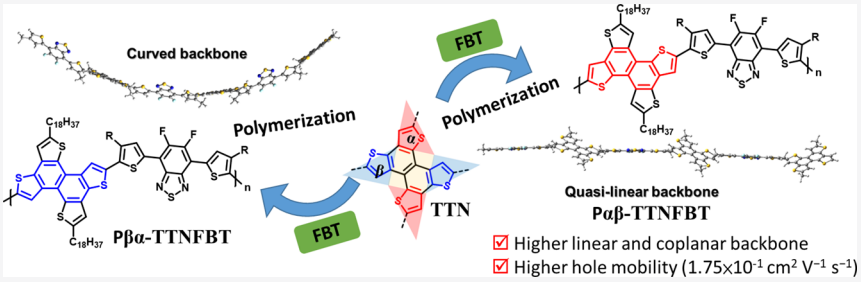

ABSTRACT: Two-dimensional alkylated ***αβ*-TTN** and ***βα*-TTN** were designed and synthesized. The cross-shaped ***αβ*-TTN** and ***βα*-TTN** moieties were polymerized to afford two isomeric polymers, **P*αβ*-TTNFBT$_{40}$** and **P*βα*-TTNFBT$_{40}$**. **P*αβ*-TTNFBT$_{40}$** using an α-aNDT unit in the main chain exhibited more red-shifted absorption and a smaller HOMO/LUMO band gap than **P*βα*-TTNFBT$_{40}$** using β-aNDT in the main chain. Compared to **P*βα*-TTNFBT$_{40}$** showing a curved backbone, density functional theory (DFT) calculations revealed that **P*αβ*-TTNFBT$_{40}$** exhibited a quasi-linear polymeric backbone that induces stronger intermolecular interactions and higher molecular ordering in the solid state. **P*αβ*-TTNFBT$_{40}$** exhibited an organic field-effect transistor (OFET) hole mobility of 1.12×10^{-2} cm^2 V^{-1} s^{-1}, which outperformed **P*βα*-TTNFBT$_{40}$** by 1 order of magnitude (1.60×10^{-3} cm^2 V^{-1} s^{-1}). Through side-chain engineering and optimization, **P*αβ*-TTNFBT$_{24}$** using a shorter 2-butyloctyl side chain further strengthened the intermolecular interactions. From grazing incidence wide-angle X-ray scattering (GIWAXS), **P*αβ*-TTNFBT$_{24}$** adopted an edge-on π–π stacking orientation in a thin film, leading to an improved mobility of 1.75×10^{-1} cm^2 V^{-1} s^{-1}, which has exceeded the mobility of the one-dimensional α-aNDT-based **PaNDTDTFBT** (4.70×10^{-2} cm^2 V^{-1} s^{-1}). This research demonstrated that the two-dimensional structure is an effective strategy to achieve higher OFET mobility, and the geometry of the main chain played a more significant role than that of the side chain in determining the physical and packing properties of polymers.

INTRODUCTION

Acenes consisting of linearly fused benzene rings have attracted tremendous research interest in terms of chemical synthesis, physical properties, and optoelectronic applications.[1−5] Fusing an acene with two terminal thiophenes to generate acenedithiophenes (AcDT) can impart multiple advantages such as improved stability, adjustable properties, diverse molecular geometry, and facile π-functionalization.[6−9] Benzodithiophene (BDT)-incorporated polymers have been the ubiquitous p-type materials to achieve highly efficient solar cells.[10−18] Anthradithiophene-based (ADT) materials also have shown high mobilities in organic field-effect transistors.[19,20] It was envisaged that naphthodithiophene (NDT) derivatives can also serve as superior building blocks for the development of polymer semiconductors used in solution-processable transistors and organic photovoltaics.[21−30] Depending on the fused junction between the thiophene and naphthalene moiety, there are two angular-shaped naphthodithiophene (aNDT) isomers denoted as α-aNDT and β-aNDT (Scheme 1). Introducing aliphatic side chains on the bare aNDT units is necessary to ensure solution processibilty.[27−34] We previously reported a synthetic methodology to regiospecifically incorporate two alkyl groups at the 4,9- or 5,10-positions of the α-aNDT and β-aNDT unit,[31] which can provide access to solution-processable aNDT-based polymers. The structural geometry of the aNDT structures played a pivotal role in governing the molecular packing and ordering of the polymers.[27] Donor–acceptor (D-A) copolymers using α-

Received: June 2, 2020
Revised: August 15, 2020
Published: September 3, 2020

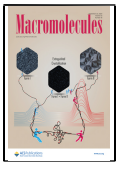

Downloaded via SYNCHROTRON RADIATION RESEARCH on January 25, 2021 at 07:57:59 (UTC).
See https://pubs.acs.org/sharingguidelines for options on how to legitimately share published articles.

ACS Publications © 2020 American Chemical Society

https://dx.doi.org/10.1021/acs.macromol.0c01297
Macromolecules 2020, 53, 7740–7748

Scheme 1. Chemical Structures of Alkylated α-aNDT and β-aNDT; Alkylated $\alpha\beta$-TTN and $\beta\alpha$-TTN; and P$\alpha\beta$-TTNFBT$_{40}$, P$\beta\alpha$-TTNFBT$_{40}$, P$\alpha\beta$-TTNFBT$_{24}$, and PaNDTDTFBT

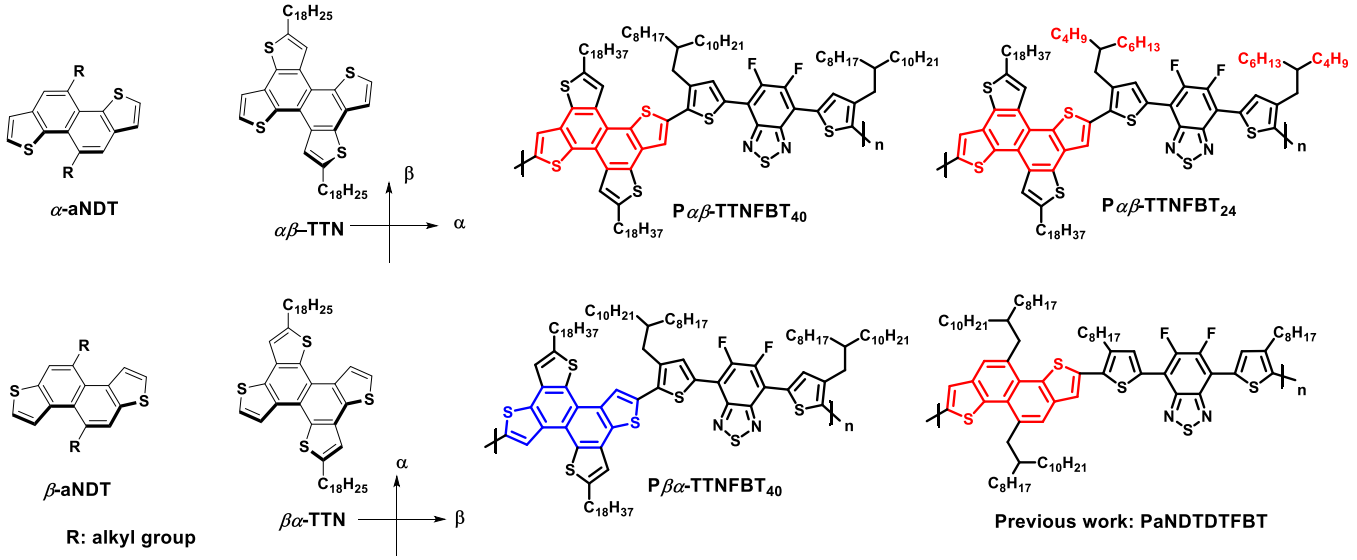

Scheme 2. Synthetic Pathway for Sn-$\alpha\beta$-TTN

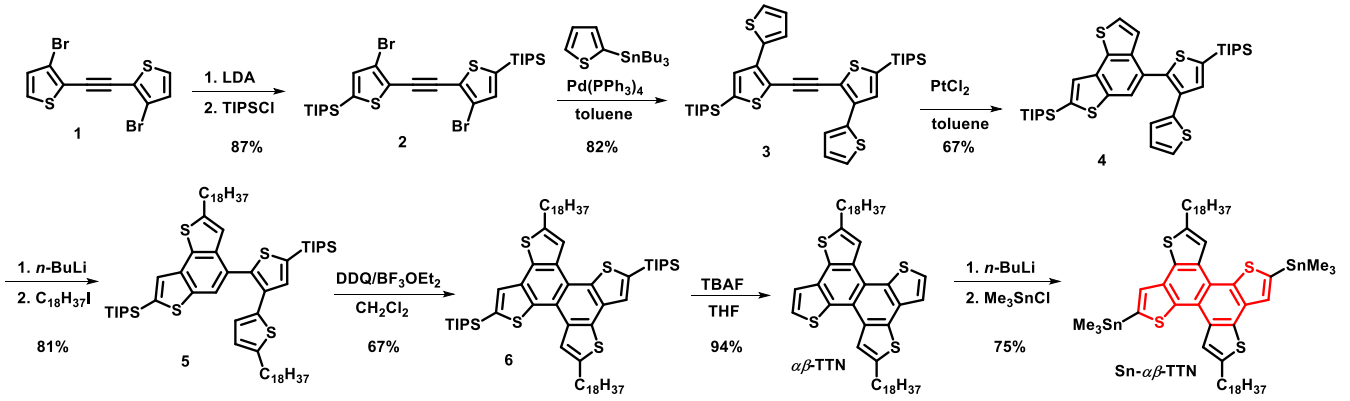

Scheme 3. Synthetic Pathway for Sn-$\beta\alpha$-TTN

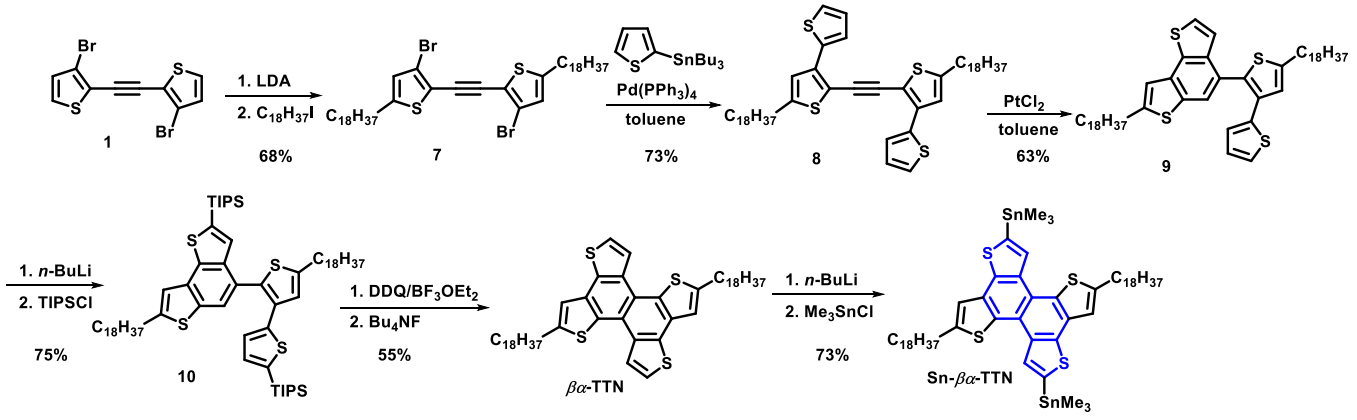

aNDT units have shown better solar cell performance and OFET mobilities than the β-aNDT-based polymers.[28] The dialkyl α-aNDT-based **PaNDTDTFBT** copolymer shown in Scheme 1 has achieved a hole mobility of 4.70×10^{-2} cm^2 V^{-1} s^{-1}.[29]

Extending a horizontal conjugation along its vertical direction to form a two-dimensional conjugated system has been demonstrated as an effective strategy to further enhance $\pi-\pi$ interactions and light-harvesting ability,[35] leading to the enhanced solar cell efficiency.[36−40] Cross-shaped tetrathienonaphthalenes (TTN)[41−44] containing two overlapping aNDT units emerge as a promising two-dimensional structure. Nevertheless, a TTN unit substituted with aliphatic side chains has never been incorporated into a donor−acceptor

https://dx.doi.org/10.1021/acs.macromol.0c01297
Macromolecules 2020, 53, 7740−7748

Scheme 4. Polymerization of P$\alpha\beta$-TTNFBT$_{40}$, P$\beta\alpha$-TTNFBT$_{40}$, and P$\alpha\beta$-TTNFBT$_{24}$

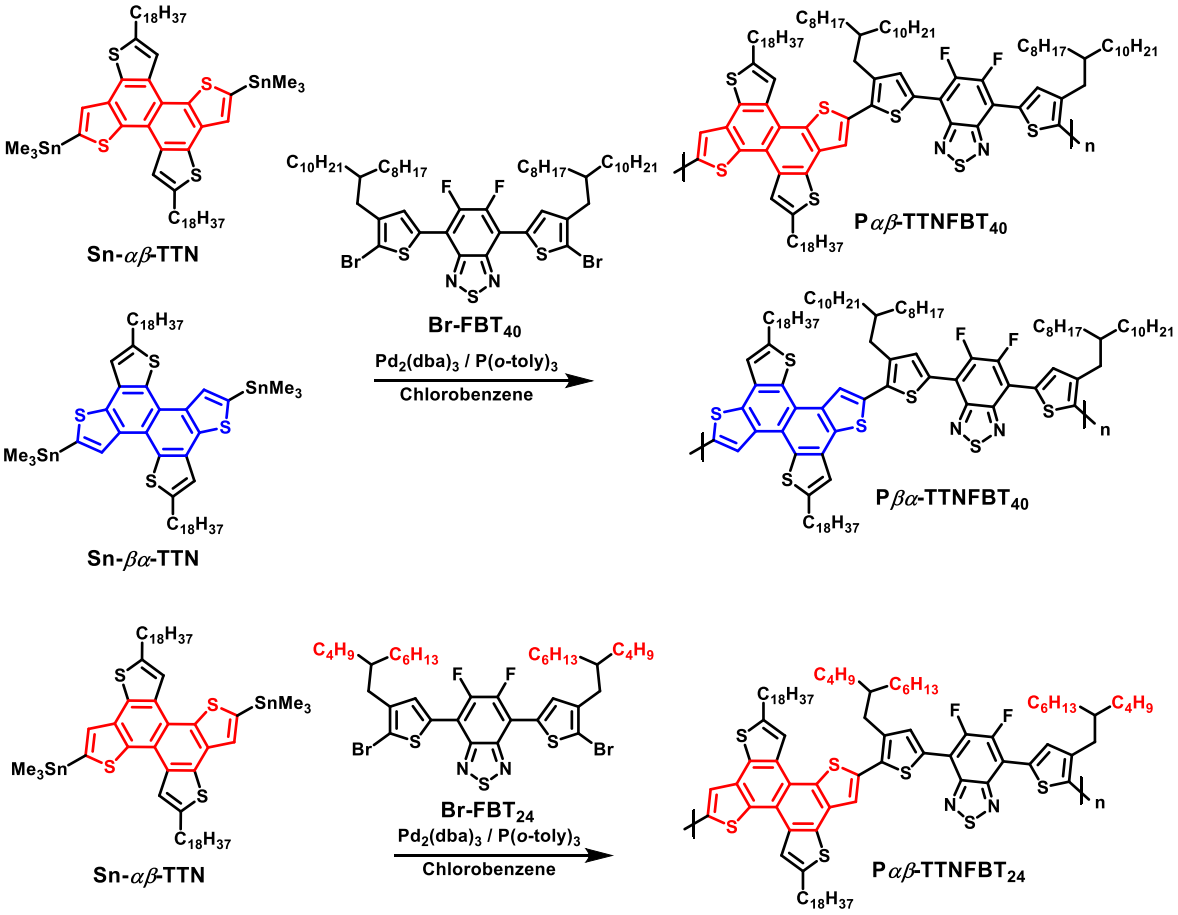

copolymer due to the lack of facile synthesis of the alkylated TTN. Herein, we designed and synthesized a new two-dimensional tetrathienonaphthalene building block (denoted as ***αβ*-TTN**) composed of a horizontally aligned α-aNDT overlapping with a vertically aligned dioctadecyl β-aNDT (Scheme 1). Reversely, an isomeric ***βα*-TTN** consisting of a horizontally aligned β-aNDT and a vertically aligned dioctadecyl α-aNDT was also developed. The two-dimensional ***αβ*-TTN** and ***βα*-TTN** were used as the donor units to make donor−acceptor conjugated copolymers. The electronic and steric effect of the two isomeric TTN structures on the polymer properties and OFET mobility will be discussed and elucidated.

RESULTS AND DISCUSSION

Synthesis. The synthetic pathway of **Sn-*αβ*-TTN** is depicted in Scheme 2. Lithiation of compound **1** by lithium diisopropylamide (LDA) followed by reacting with triisopropylsilyl chloride (TIPSCl) afforded compound **2**.[45] The Stille coupling reaction of dibrominated compound **2** with 2-(tributylstannyl) thiophene resulted in compound **3**.[42] $PtCl_2$-catalyzed intramolecular cyclization of compound **3** formed the single cyclized compound **4**.[44] Lithiation of compound **4** by *n*-BuLi to react with 1-iodooctadecane yielded compound **5**. Scholl-type oxidative cyclization in the presence of DDQ/BF_3OEt_2 furnished compound **6**, which was desilylated by tetrabutyl ammonium fluoride (TBAF) to afford ***αβ*-TTN**. Stannylation of ***αβ*-TTN** by *n*-BuLi/Me_3SnCl yielded the target **Sn-*αβ*-TTN** monomer. By reversing the sequence of installing TIPS and octadecyl groups, the isomeric **Sn-*βα*-TTN** counterpart was synthesized in a similar manner shown in Scheme 3.

The two-dimensional **Sn-*αβ*-TTN** and **Sn-*βα*-TTN** monomers were copolymerized with a 4,7-bis(5-bromo-4-alkylthiophen-2-yl)-5,6-difluorobenzo[c][1,2,5]-thiadiazole (symbolized as FBT) monomer using 2-octyldodecyl as the side chains[29] to form two isomeric donor−acceptor copolymers, **P*αβ*-TTNFBT$_{40}$** and **P*βα*-TTNFBT$_{40}$** (40 is the total carbon number on the FBT moiety), respectively. To further investigate the side-chain effect, **Sn-*αβ*-TTN** was further polymerized with the FBT monomer with shorter branched side chains (2-butyloctyl)[46] to afford **P*αβ*-TTNFBT$_{24}$** (Scheme 4). All polymers were purified via Soxhlet extraction by acetone, hexane, and THF sequentially. The molecular weights of **P*αβ*-TTNFBT$_{40}$** and **P*βα*-TTNFBT$_{40}$** were determined by gel permeation chromatography (GPC) to be 70.4 (PDI = 1.3) and 29.4 KDa (PDI = 1.5), respectively. **P*αβ*-TTNFBT$_{24}$** showed a lower molecular weight of 54.1 KDa (PDI = 1.2) due to the reduced solubility.

Thermal Properties. Thermal properties and the GPC data are summarized in Table 1. Thermogravimetric plots are shown in Figure S1. The thermal decomposition temperatures (T_d) were determined to be 380, 382, and 381 °C. The differential scanning calorimetry measurement of the three polymers showed no obvious thermal transitions (Figure S2).

UV−Vis Absorption Spectroscopy. The UV−vis absorption spectra of the TTN-based polymers in chlorobenzene (CB) solution and thin films are shown in Figure 1 and

https://dx.doi.org/10.1021/acs.macromol.0c01297
Macromolecules 2020, 53, 7740−7748

Table 1. Molecular Weight and Thermal Properties of the Copolymers

polymer	M_n (kDa, g/mol)[a]	PDI (M_w/M_n)[a]	T_d (°C)[b]
Pαβ-TTNFBT$_{40}$	70.4	1.3	380
Pβα-TTNFBT$_{40}$	29.4	1.5	382
Pαβ-TTNFBT$_{24}$	54.1	1.2	381

[a]Determined by GPC in THF based on polystyrene standards. [b]Decomposition temperature based on 5% weight loss determined by thermal gravimetric analysis (TGA).

Table 2. Optical Properties of Pαβ-TTNFBT$_{40}$, Pβα-TTNFBT$_{40}$, and Pαβ-TTNFBT$_{24}$

	λ_{max} (nm)			
polymer	CB	film	λ_{onset} (nm)	E_g^{opt} (eV)[a]
Pαβ-TTNFBT$_{40}$	592	630	734	1.69
Pβα-TTNFBT$_{40}$	540	571	696	1.78
Pαβ-TTNFBT$_{24}$	594, 638	644	745	1.66

[a]$E_g^{opt} = 1240/\lambda_{onset}$.

summarized in Table 2. The absorption in the shorter-wavelength region corresponds to the localized $\pi-\pi^*$ transition (LT), and the longer-wavelength region originates from intramolecular charge transfer (ICT) that occurs from donor to acceptor moieties of the polymers. **Pβα-TTNFBT$_{40}$** showed an absorption λ_{max} at 540 nm, while the isomeric **Pαβ-TTNFBT$_{40}$** exhibited a much more red-shifted λ_{max} at 592 nm in solution, indicating that **Pαβ-TTNFBT$_{40}$** using the α-aNDT moiety as the main chain has better effective conjugation than **Pβα-TTNFBT$_{40}$** using the isomeric β-aNDT as the main chain. Compared to **Pαβ-TTNFBT$_{40}$**, **Pαβ-TTNFBT$_{24}$** with the identical main chain composition but the shorter branched side chains (2-butyloctyl) exhibited a slightly bathochromic absorption profile with a vibronic shoulder, suggesting the strengthened intermolecular interactions as a result of the reduced steric hindrance of the side chains. The absorption spectra of the polymers were red-shifted in the thin film states due to the closer intermolecular packing. **Pαβ-TTNFBT$_{24}$** particularly showed the pronounced band broadening in the thin-film state, indicative of a better π-stacking.

Temperature-dependent absorption spectra (Figure 2) of **Pαβ-TTNFBT$_{40}$** and **Pβα-TTNFBT$_{40}$** from 25 to 140 °C were carried out in *o*DCB. When temperature increases, the absorption is gradually blue-shifted, indicating that there is a certain aggregation existing at low temperature. The λ_{max} of **Pαβ-TTNFBT$_{40}$** is blue-shifted by 20 nm from 25 to 140 °C, which is larger than that of **Pβα-TTNFBT$_{40}$** (15 nm). This result suggested that **Pαβ-TTNFBT$_{40}$** has stronger intermolecular aggregations in solution. The thin-film state absorption spectra of **Pαβ-TTNFBT$_{40}$** (λ_{max} at 630 nm) and **Pαβ-TTNFBT$_{24}$** (λ_{max} at 571 nm) are further red-shifted. DFT calculations revealed that **Pαβ-TTNFBT$_{40}$** exhibited a quasi-linear polymeric backbone, which induces stronger intermolecular interactions and higher molecular ordering in the solid state.

Electrochemical Properties. The electrochemical properties were measured by cyclic voltammetry and shown in Figure 3 and Table 3. The highest occupied molecular orbital (HOMO) and lowest unoccupied molecular orbital (LUMO) energy level of **Pαβ-TTNFBT$_{40}$** were estimated to be −5.72 and −3.59 eV, respectively. **Pβα-TTNFBT$_{40}$** exhibited a lower-lying HOMO energy level of −5.75 eV and a higher-lying LUMO of −3.49 eV, leading to a wider band gap of 2.26 eV. Because of the identical main-chain backbone, **Pαβ-TTNFBT$_{24}$** showed similar HOMO/LUMO levels (−5.68 eV/−3.56 eV) to **Pαβ-TTNFBT$_{40}$**. The trend of the electrochemical band gap is qualitatively consistent with that of the optical band gap.

Theoretical Calculations. To investigate the geometrical effect of two isomeric **αβ-TTN** and **βα-TTN** units on the polymeric conformation, density functional theory (DFT) was exploited to calculate the optimized geometry of **αβ-TTNFBT** and **βα-TTNFBT** trimers (symbolized as **tri-αβ-TTNFBT** and **tri-βα-TTNFBT**) with the Gaussian09 suite at B3LYP/6-311(d,p). To simplify the calculation, all the alkyl side chains were replaced with methyl groups. As shown in Figure 4, **tri-βα-TTNFBT** shows a relatively curved backbone with the angle between three sulfur atoms in the benzothiadiazole units to be 147.9°, whereas **tri-αβ-TTNFBT** has a quasi-linear backbone (the angle is 173.6°) that tends to induce a more ordered packing structure. The polymeric conformation difference mainly originates from the geometrical shape of **αβ-TTN** (α-aNDT as the main chain) and **βα-TTN** (β-aNDT as the main chain). These conformational results are consistent with the relevant systems in the literatures.[28]

Transistor Characterization. The organic field-effect transistors (OFETs) were fabricated with the bottom-gate/top-contact structure to measure the hole mobility of the polymers. The self-assembly monolayer of octadecyltrichlorosilane (ODTS) was introduced to modify the SiO_2 dielectric gate. The OFET device parameters are summarized in Table 4, while the output characteristics and transfer characteristics are shown in Figure 5. **Pαβ-TTNFBT$_{40}$** exhibited a hole mobility of 1.12×10^{-2} cm^2 V^{-1} s^{-1}, which greatly outperformed **Pβα-**

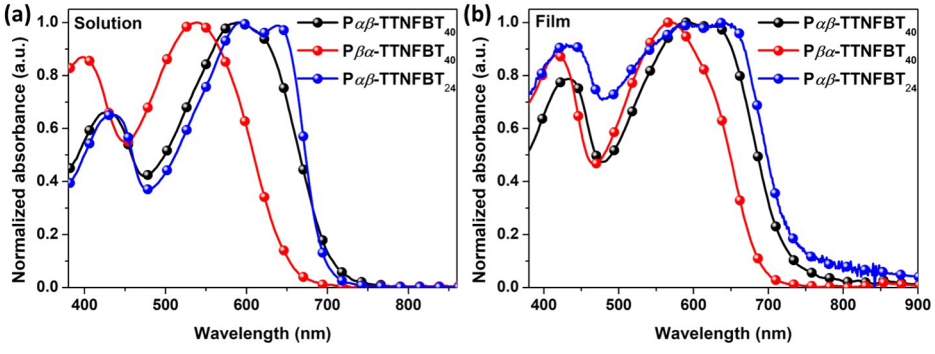

Figure 1. Absorption spectra of **Pαβ-TTNFBT$_{40}$**, **Pβα-TTNFBT$_{40}$**, and **Pαβ-TTNFBT$_{24}$** in (a) CB solution and the (b) thin-film state.

https://dx.doi.org/10.1021/acs.macromol.0c01297
Macromolecules 2020, 53, 7740−7748

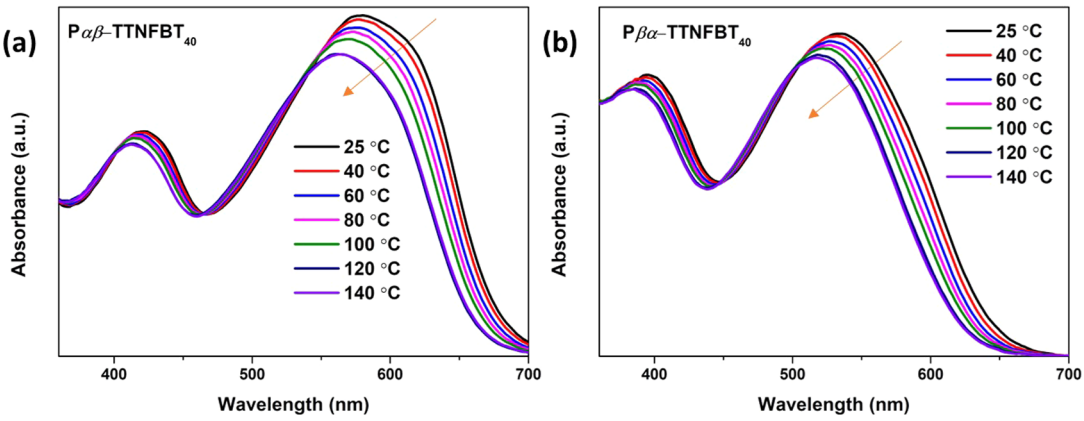

Figure 2. Temperature-dependent absorption spectra of (a) **Pαβ-TTNFBT$_{40}$** and (b) **Pβα-TTNFBT$_{40}$** in *o*DCB solution from 25 to 140 °C.

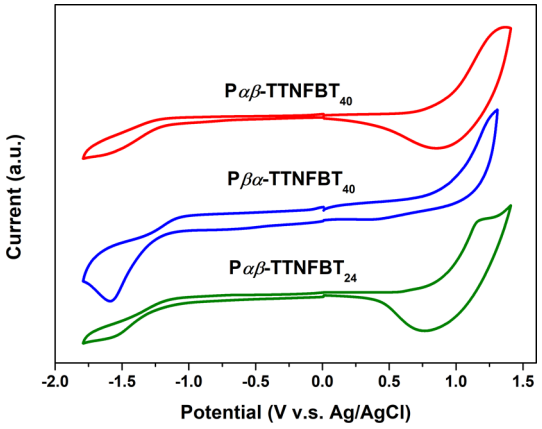

Figure 3. Cyclic voltammograms of **Pαβ-TTNFBT$_{40}$**, **Pβα-TTNFBT$_{40}$**, and **Pαβ-TTNFBT$_{24}$** at a ramping rate of 10 mV/s.

Table 3. Electrochemical Properties of Pαβ-TTNFBT$_{40}$, Pβα-TTNFBT$_{40}$, and Pαβ-TTNFBT$_{24}$

polymer	HOMO (eV)[a]	LUMO (eV)[b]	E_g^{ele} (eV)[c]
Pαβ-TTNFBT$_{40}$	−5.72	−3.59	2.13
Pβα-TTNFBT$_{40}$	−5.75	−3.49	2.26
Pαβ-TTNFBT$_{24}$	−5.68	−3.56	2.12

[a]The HOMO energy levels obtained by the equation HOMO = $-(E_{ox}^{onset} - E_{ferrocene}^{onset} + 4.8)$ eV. [b]The LUMO energy levels obtained by the equation LUMO = $-(E_{red}^{onset} - E_{ferrocene}^{onset} + 4.8)$ eV. [c]E_g^{ele} = LUMO − HOMO.

TTNFBT$_{40}$ with a mobility of 1.60×10^{-3} cm^2 V^{-1} s^{-1} by 1 order of magnitude. **Pαβ-TTNFBT$_{24}$** with shorter branched side chains further improved the mobility to 1.75×10^{-1} cm^2 V^{-1} s^{-1}. The higher mobility of **Pαβ-TTNFBT** polymers is

Table 4. OFET Device Parameters of Pαβ-TTNFBT$_{40}$, Pβα-TTNFBT$_{40}$, and Pαβ-TTNFBT$_{24}$

polymer	annealing temperature (°C)	μ_h (cm^2 V^{-1} s^{-1})	$I_{on/off}$	V_{th} (V)
Pαβ-TTNFBT$_{40}$	200	1.12×10^{-2}	1.64×10^3	−18.8
Pβα-TTNFBT$_{40}$	180	1.60×10^{-3}	2.82×10^5	−25.7
Pαβ-TTNFBT$_{24}$	180	1.75×10^{-1}	7.74×10^5	−49.9

highly associated with its more linear polymer backbone. It should be noted that this value is higher than that of **PaNDTDTFBT** (4.70×10^{-2} cm^2 V^{-1} s^{-1}) using one-dimensional *α*-aNDT in the backbone.[29] The 1D and 2D comparison indicated that the two-dimensional ***αβ*-TTN** moiety is indeed beneficial to improving the charge mobility. It should be also pointed out that the molecular weight difference might have a minor influence on the OFET charge mobility.

GIWAXS. Grazing incidence wide-angle X-ray scattering (GIWAXS) was employed to examine the molecular orientation of the polymer in thin films. All the polymeric solutions were prepared in chlorobenzene and spin-coated on the ODTS-modified Si/SiO$_2$ wafers followed by thermal annealing at 180 or 200 °C for 10 min. 2D GIWAXS images and the corresponding one-dimensional out-of-plane (q_z) and in-plane (q_{xy}) diffraction patterns of the polymer thin films are shown in Figures 6 and 7, respectively. **Pαβ-TTNFBT$_{40}$** exhibited a strong (010) signal at q_z = 1.77 Å^{-1} corresponding to periodic $\pi-\pi$ stacking with a distance (d_π) of ca. 3.55 Å, suggesting that the polymer adopted a face-on orientation. Nevertheless, the isomeric **Pβα-TTNFBT$_{40}$** did not show

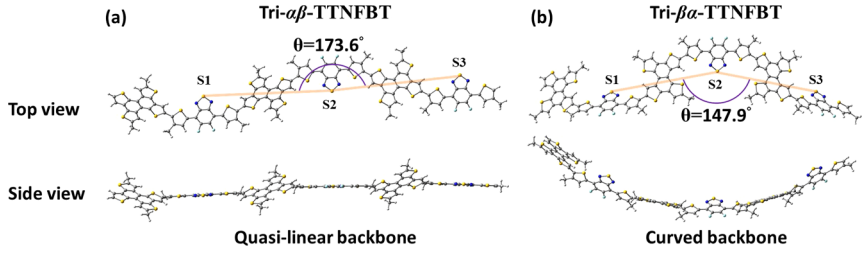

Figure 4. Top view and side view of the optimized geometries for (a) **tri-αβTTNFBT** and (b) **tri-βαTTNFBT** calculated by the B3LYP/6-311G(d,p) level. The curvature angles were calculated from the three sulfur atoms on FBT moieties.

https://dx.doi.org/10.1021/acs.macromol.0c01297
Macromolecules 2020, 53, 7740−7748

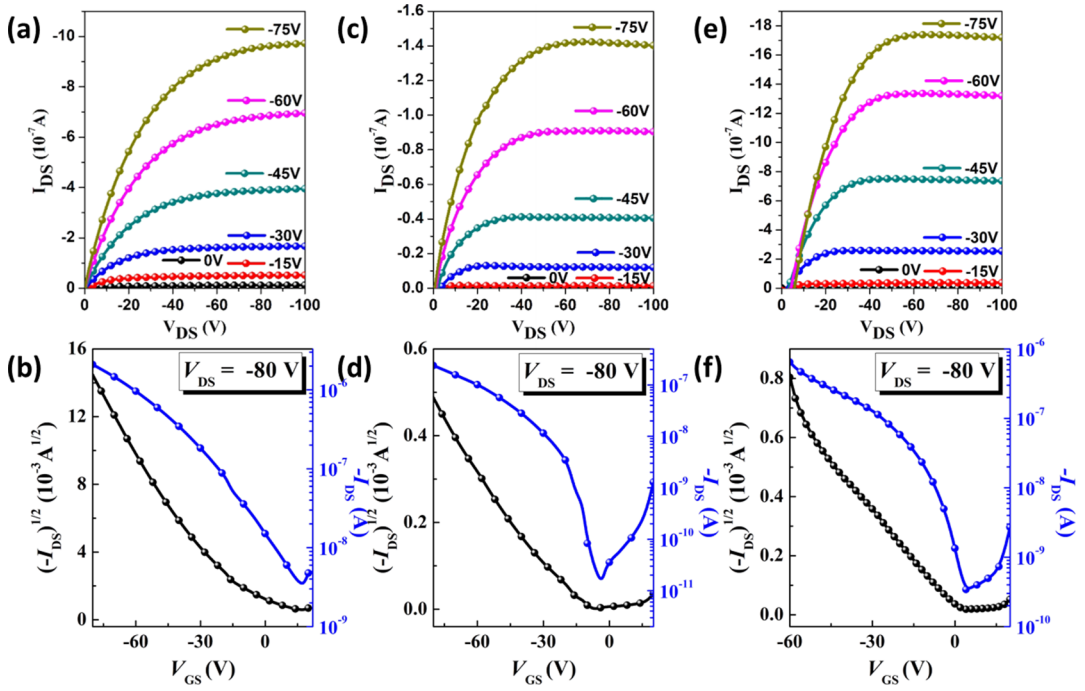

Figure 5. Typical output curves and transfer plots of the OFET devices based on (a, b) **Pαβ-TTNFBT$_{40}$**, (c, d) **Pβα-TTNFBT$_{40}$**, and (e, f) **Pαβ-TTNFBT$_{24}$**.

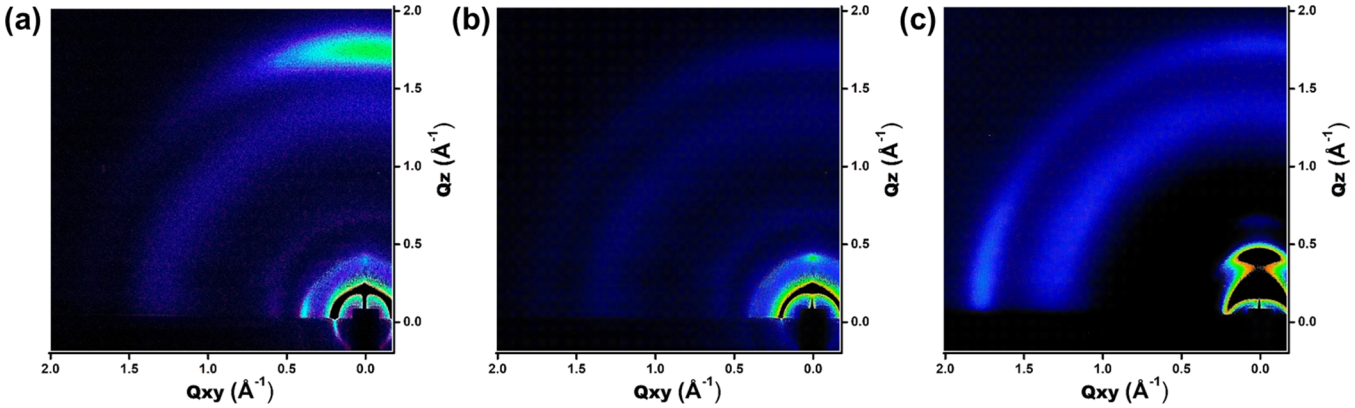

Figure 6. 2D GIWAXS images of (a) **Pαβ-TTNFBT$_{40}$**, (b) **Pβα-TTNFBT$_{40}$**, and (c) **Pαβ-TTNFBT$_{24}$** thin films.

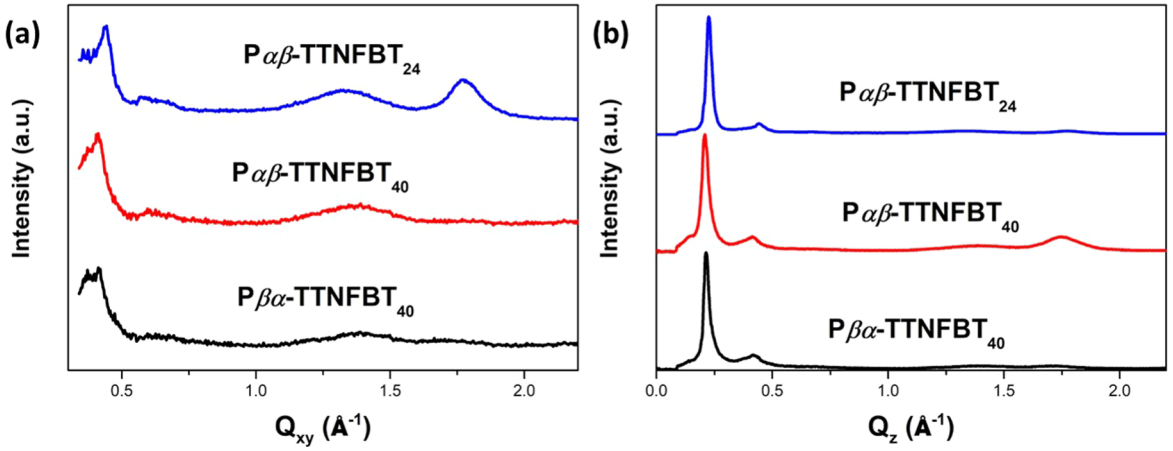

Figure 7. 1D GIWAXS profiles of (a) in-plane and (b) out-of-plane directions from the corresponding 2D GIWAXS images.

typical $\pi-\pi$ stacking diffraction in either the q_z or q_{xy} direction, indicating that **Pβα-TTNFBT$_{40}$** cannot form ordered molecular stacking in the thin-film state. **Pαβ-TTNFBT$_{40}$** has a more linear and planar conjugated backbone, thus facilitating the

https://dx.doi.org/10.1021/acs.macromol.0c01297
Macromolecules 2020, 53, 7740−7748

intermolecular packing. Interestingly, **Pαβ-TTNFBT$_{24}$** exhibited a stronger $\pi-\pi$ stacking signal in the in-plane direction (d_π = 3.59 Å), meaning that **Pαβ-TTNFBT$_{24}$** predominately adopted an edge-on orientation, which is believed to be favorable for horizontal charge transportation in an OFET device.[47,48] Furthermore, **Pαβ-TTNFBT$_{40}$** and **Pβα-TTNFBT$_{40}$** films exhibited out-of-plane (h00) signals assigned to lamellar spacings (d_1) of ca. 30.60 and 29.60 Å, respectively, which are ascribed to side-chain interdigitation.[49] Consequently, **Pαβ-TTNFBT$_{24}$** with the shortened alkyl side chains resulted in a reduced lamellar spacing of 28.12 Å. The polymer packing dictated by the GIWAXS analysis is fully consistent with the OFET charge mobilities.

CONCLUSIONS

In summary, we designed two synthetic pathways to prepare two two-dimensional dioctadodecyl tetrathienonaphthalenes, ***αβ*-TTN** and ***βα*-TTN**. The cross-shaped $\alpha\beta$-TTN contains a horizontally aligned α-aNDT and a vertically aligned dioctadodecyl β-aNDT, whereas $\beta\alpha$-TTN has a vertically aligned β-aNDT and a horizontally aligned dioctadodecyl α-aNDT. The distannylated ***αβ*-TTN** and ***βα*-TTN** units were polymerized with an FBT monomer to form two isomeric polymers **Pαβ-TTNFBT$_{40}$** and **Pβα-TTNFBT$_{40}$**. **Pαβ-TTNFBT$_{40}$** uses α-aNDT moieties as the main chain and β-aNDT moieties as the side chain, whereas **Pβα-TTNFBT$_{40}$** has the opposite arrangement. **Pαβ-TTNFBT$_{40}$** with α-aNDT moieties in the main chain showed better conjugation and a quasi-linear polymeric backbone, which induces more ordered molecular packing. As a result, **Pαβ-TTNFBT$_{40}$** exhibited a hole mobility of 1.12×10^{-2} cm^2 V^{-1} s^{-1}, which outperformed **Pβα-TTNFBT$_{40}$** by 1 order of magnitude (1.60×10^{-3} cm^2 V^{-1} s^{-1}). **Pαβ-TTNFBT$_{24}$** with shorter branched side chains adopted an edge-on orientation in a thin film to further improve the mobility to 1.75×10^{-1} cm^2 V^{-1} s^{-1}. This value has exceeded the mobility obtained from the one-dimensional α-aNDT-based **PaNDTDTFBT** (4.70×10^{-2} cm^2 V^{-1} s^{-1}).

ASSOCIATED CONTENT

Supporting Information

The Supporting Information is available free of charge at https://pubs.acs.org/doi/10.1021/acs.macromol.0c01297.

General measurements, TGA/DSC curves, fabrication and characterization of OFET devices, synthetic procedures, NMR spectra, and computational details (PDF)

AUTHOR INFORMATION

Corresponding Author

Yen-Ju Cheng − *Department of Applied Chemistry and Center for Emergent Functional Matter Science, National Chiao Tung University, Hsinchu 30010, Taiwan;* orcid.org/0000-0003-0780-4557; Email: yjcheng@nctu.edu.tw

Authors

Huai-Hsuan Liu − *Department of Applied Chemistry, National Chiao Tung University, Hsinchu 30010, Taiwan*

Shao-Ling Chang − *Department of Applied Chemistry, National Chiao Tung University, Hsinchu 30010, Taiwan*

Kuo-Hsiu Huang − *Department of Applied Chemistry, National Chiao Tung University, Hsinchu 30010, Taiwan*

Fong-Yi Cao − *Department of Applied Chemistry, National Chiao Tung University, Hsinchu 30010, Taiwan*

Kuang-Yi Cheng − *Department of Applied Chemistry, National Chiao Tung University, Hsinchu 30010, Taiwan*

Han-Sheng Sun − *Institute of Polymer Science and Engineering, National Taiwan University, Taipei 10617, Taiwan*

Yu-Ying Lai − *Institute of Polymer Science and Engineering, National Taiwan University, Taipei 10617, Taiwan;* orcid.org/0000-0002-1921-6923

Complete contact information is available at: https://pubs.acs.org/10.1021/acs.macromol.0c01297

Notes

The authors declare no competing financial interest.

ACKNOWLEDGMENTS

This work is supported by the Ministry of Science and Technology, Taiwan (grant no. MOST107-3017-F-009-003 and 107-2628-M-009-003-MY3) and the Ministry of Education, Taiwan (SPROUT Project-Center for Emergent Functional Matter Science of National Chiao Tung University). We thank the National Center of High-Performance Computing (NCHC) in Taiwan for computer time and facilities. We also thank the National Synchrotron Radiation Research Center (NSRRC) and Dr. U-Ser Jeng at BL23A station for the help with the GIWAXS experiments.

REFERENCES

(1) Cheng, Y.-J.; Yang, S.-H.; Hsu, C.-S. Synthesis of Conjugated Polymers for Organic Solar Cell Applications. *Chem. Rev.* **2009**, *109*, 5868−5923.

(2) Wu, J.-S.; Cheng, S.-W.; Cheng, Y.-J.; Hsu, C.-S. Donor−acceptor conjugated polymers based on multifused ladder-type arenes for organic solar cells. *Chem. Soc. Rev.* **2015**, *44*, 1113−1154.

(3) Zhou, H.; Yang, L.; You, W. Rational Design of High Performance Conjugated Polymers for Organic Solar Cells. *Macromolecules* **2012**, *45*, 607−632.

(4) Lee, C.; Lee, S.; Kim, G.-U.; Lee, W.; Kim, B. J. Recent Advances, Design Guidelines, and Prospects of All-Polymer Solar Cells. *Chem. Rev.* **2019**, *119*, 8028−8086.

(5) Bathula, C.; Kim, M.; Song, C. E.; Shin, W. S.; Hwang, D.-H.; Lee, J.-C.; Kang, I.-N.; Lee, S. K.; Park, T. Concentration-Dependent Pyrene-Driven Self-Assembly in Benzo[1,2-b:4,5-b′]dithiophene (BDT)−Thienothiophene (TT)−Pyrene Copolymers. *Macromolecules* **2015**, *48*, 3509−3515.

(6) Takimiya, K.; Shinamura, S.; Osaka, I.; Miyazaki, E. Thienoacene-Based Organic Semiconductors. *Adv. Mater.* **2011**, *23*, 4347−4370.

(7) Nakano, M.; Shinamura, S.; Sugimoto, R.; Osaka, I.; Miyazaki, E.; Takimiya, K. Borylation on Benzo[1,2-b:4,5-b′]- and Naphtho[1,2-b:5,6-b′]dichalcogenophenes: Different Chalcogene Atom Effects on Borylation Reaction Depending on Fused Ring Structure. *Org. Lett.* **2012**, *14*, 5448−5451.

(8) Nakano, M.; Niimi, K.; Miyazaki, E.; Osaka, I.; Takimiya, K. Isomerically Pure Anthra[2,3-b:6,7-b′]-difuran (anti-ADF), −dithiophene (anti-ADT), and -diselenophene (anti-ADS): Selective Synthesis, Electronic Structures, and Application to Organic Field-Effect Transistors. *J. Org. Chem.* **2012**, *77*, 8099−8111.

(9) Goetz, K. P.; Li, Z.; Ward, J. W.; Bougher, C.; Rivnay, J.; Smith, J.; Conrad, B. R.; Parkin, S. R.; Anthopoulos, T. D.; Salleo, A.; Anthony, J. E.; Jurchescu, O. D. Effect of Acene Length on Electronic Properties in 5-, 6-, and 7-Ringed Heteroacenes. *Adv. Mater.* **2011**, *23*, 3698−3703.

(10) Huo, L.; Hou, J.; Zhang, S.; Chen, H.-Y.; Yang, Y. A Polybenzo[1,2-b:4,5-b′]dithiophene Derivative with Deep HOMO

Level and Its Application in High-Performance Polymer Solar Cells. *Angew. Chem., Int. Ed.* **2010**, *49*, 1500−1503.
(11) Ye, L.; Jiang, W.; Zhao, W.; Zhang, S.; Qian, D.; Wang, Z.; Hou, J. Selecting a Donor Polymer for Realizing Favorable Morphology in Efficient Non-fullerene Acceptor-based Solar Cells. *Small* **2014**, *10*, 4658−4663.
(12) Hou, J.; Park, M.-H.; Zhang, S.; Yao, Y.; Chen, L.-M.; Li, J.-H.; Yang, Y. Bandgap and Molecular Energy Level Control of Conjugated Polymer Photovoltaic Materials Based on Benzo[1,2-b:4,5-b′]-dithiophene. *Macromolecules* **2008**, *41*, 6012−6018.
(13) Sun, C.; Pan, F.; Qiu, B.; Qin, S.; Chen, S.; Shang, Z.; Meng, L.; Yang, C.; Li, Y. D−A Copolymer Donor Based on Bithienyl Benzodithiophene D-Unit and Monoalkoxy Bifluoroquinoxaline A-Unit for High-Performance Polymer Solar Cells. *Chem. Mater.* **2020**, *32*, 3254−3261.
(14) Kim, J.-H.; Song, C. E.; Shin, N.; Kang, H.; Wood, S.; Kang, I.-N.; Kim, B. J.; Kim, B.; Kim, J.-S.; Shin, W. S.; Hwang, D.-H. High-Crystalline Medium-Band-Gap Polymers Consisting of Benzodithiophene and Benzotriazole Derivatives for Organic Photovoltaic Cells. *ACS Appl. Mater. Interfaces* **2013**, *5*, 12820−12831.
(15) Kim, T.; Choi, J.; Kim, H. J.; Lee, W.; Kim, B. J. Comparative Study of Thermal Stability, Morphology, and Performance of All-Polymer, Fullerene−Polymer, and Ternary Blend Solar Cells Based on the Same Polymer Donor. *Macromolecules* **2017**, *50*, 6861−6871.
(16) Park, J. S.; Choi, N.; Lee, C.; Lee, S.; Ha, J.-W.; Hwang, D.-H.; Kim, B. J. Elucidating Roles of Polymer Donor Aggregation in All-Polymer and Non-Fullerene Small-Molecule−Polymer Solar Cells. *Chem. Mater.* **2020**, *32*, 3585−3596.
(17) Kang, T. E.; Kim, T.; Wang, C.; Yoo, S.; Kim, B. J. Poly(benzodithiophene) Homopolymer for High-Performance Polymer Solar Cells with Open-Circuit Voltage of Near 1 V: A Superior Candidate To Substitute for Poly(3-hexylthiophene) as Wide Bandgap Polymer. *Chem. Mater.* **2015**, *27*, 2653−2658.
(18) Liu, P.; Zhang, K.; Liu, F.; Jin, Y.; Liu, S.; Russell, T. P.; Yip, H.-L.; Huang, F.; Cao, Y. Effect of Fluorine Content in Thienothiophene-Benzodithiophene Copolymers on the Morphology and Performance of Polymer Solar Cells. *Chem. Mater.* **2014**, *26*, 3009−3017.
(19) Lehnherr, D.; Waterloo, A. R.; Goetz, K. P.; Payne, M. M.; Hampel, F.; Anthony, J. E.; Jurchescu, O. D.; Tykwinski, R. R. Isomerically Pure syn-Anthradithiophenes: Synthesis, Properties, and FET Performance. *Org. Lett.* **2012**, *14*, 3660−3663.
(20) Wu, J.-S.; Lin, C.-T.; Wang, C.-L.; Cheng, Y.-J.; Hsu, C.-S. New Angular-Shaped and Isomerically Pure Anthradithiophene with Lateral Aliphatic Side Chains for Conjugated Polymers: Synthesis, Characterization, and Implications for Solution-Prossessed Organic Field-Effect Transistors and Photovoltaics. *Chem. Mater.* **2012**, *24*, 2391−2399.
(21) Osaka, I.; Abe, T.; Shinamura, S.; Takimiya, K. Impact of Isomeric Structures on Transistor Performances in Naphthodithiophene Semiconducting Polymers. *J. Am. Chem. Soc.* **2011**, *133*, 6852−6860.
(22) Shinamura, S.; Osaka, I.; Miyazaki, E.; Nakao, A.; Yamagishi, M.; Takeya, J.; Takimiya, K. Linear- and Angular-Shaped Naphthodithiophenes: Selective Synthesis, Properties, and Application to Organic Field-Effect Transistors. *J. Am. Chem. Soc.* **2011**, *133*, 5024−5035.
(23) Zhu, X.; Fang, J.; Lu, K.; Zhang, J.; Zhu, L.; Zhao, Y.; Shuai, Z.; Wei, Z. Naphtho[1,2-b:5,6-b′]dithiophene Based Two-Dimensional Conjugated Polymers for Highly Efficient Thick-Film Inverted Polymer Solar Cells. *Chem. Mater.* **2014**, *26*, 6947−6954.
(24) Osaka, I.; Kakara, T.; Takemura, N.; Koganezawa, T.; Takimiya, K. Naphthodithiophene−Naphthobisthiadiazole Copolymers for Solar Cells: Alkylation Drives the Polymer Backbone Flat and Promotes Efficiency. *J. Am. Chem. Soc.* **2013**, *135*, 8834−8837.
(25) Hwang, M. C.; Jang, J.-W.; An, T. K.; Park, C. E.; Kim, Y.-H.; Kwon, S.-K. Synthesis and Characterization of New Thermally Stable Poly(naphthodithiophene) Derivatives and Applications for High-Performance Organic Thin Film Transistors. *Macromolecules* **2012**, *45*, 4520−4528.
(26) Osaka, I.; Abe, T.; Shimawaki, M.; Koganezawa, T.; Takimiya, K. Naphthodithiophene-Based Donor−Acceptor Polymers: Versatile Semiconductors for OFETs and OPVs. *ACS Macro Lett.* **2012**, *1*, 437−440.
(27) Chiou, D.-Y.; Cao, F.-Y.; Hsu, J.-Y.; Tsai, C.-E.; Lai, Y.-Y.; Jeng, U. S.; Zhang, J.; Yan, H.; Su, C.-J.; Cheng, Y.-J. Synthesis and side-chain isomeric effect of 4,9−/5,10-dialkylated-β-angular-shaped naphthodithiophenes-based donor−acceptor copolymers for polymer solar cells and field-effect transistors. *Polym. Chem.* **2017**, *8*, 2334−2345.
(28) Cheng, S.-W.; Chiou, D.-Y.; Tsai, C.-E.; Liang, W.-W.; Lai, Y.-Y.; Hsu, J.-Y.; Hsu, C.-S.; Osaka, I.; Takimiya, K.; Cheng, Y.-J. Angular-Shaped 4,9-Dialkyl α- and β-Naphthodithiophene-Based Donor−Acceptor Copolymers: Investigation of Isomeric Structural Effects on Molecular Properties and Performance of Field-Effect Transistors and Photovoltaics. *Adv. Funct. Mater.* **2015**, *25*, 6131−6143.
(29) Cheng, S.-W.; Tsai, C.-E.; Liang, W.-W.; Chen, Y.-L.; Cao, F.-Y.; Hsu, C.-S.; Cheng, Y.-J. Angular-Shaped 4,9-Dialkylnaphthodithiophene-Based Donor−Acceptor Copolymers for Efficient Polymer Solar Cells and High-Mobility Field-Effect Transistors. *Macromolecules* **2015**, *48*, 2030−2038.
(30) Loser, S.; Bruns, C. J.; Miyauchi, H.; Ortiz, R. P.; Facchetti, A.; Stupp, S. I.; Marks, T. J. A Naphthodithiophene-Diketopyrrolopyrrole Donor Molecule for Efficient Solution-Processed Solar Cells. *J. Am. Chem. Soc.* **2011**, *133*, 8142−8145.
(31) Cheng, S.-W.; Chiou, D.-Y.; Lai, Y.-Y.; Yu, R.-H.; Lee, C.-H.; Cheng, Y.-J. Synthesis and Molecular Properties of Four Isomeric Dialkylated Angular-Shaped Naphthodithiophenes. *Org. Lett.* **2013**, *15*, 5338−5341.
(32) Osaka, I.; Houchin, Y.; Yamashita, M.; Kakara, T.; Takemura, N.; Koganezawa, T.; Takimiya, K. Contrasting Effect of Alkylation on the Ordering Structure in Isomeric Naphthodithiophene-Based Polymers. *Macromolecules* **2014**, *47*, 3502−3510.
(33) Shi, S.; Xie, X.; Jiang, P.; Chen, S.; Wang, L.; Wang, M.; Wang, H.; Li, X.; Yu, G.; Li, Y. Naphtho[1,2-b:5,6-b′]dithiophene-Based Donor−Acceptor Copolymer Semiconductors for High-Mobility Field-Effect Transistors and Efficient Polymer Solar Cells. *Macromolecules* **2013**, *46*, 3358−3366.
(34) Sanjaykumar, S. R.; Badgujar, S.; Song, C. E.; Shin, W. S.; Moon, S.-J.; Kang, I.-N.; Lee, J.; Cho, S.; Lee, S. K.; Lee, J.-C. Synthesis and Characterization of a Novel Naphthodithiophene-Based Copolymer for Use in Polymer Solar Cells. *Macromolecules* **2012**, *45*, 6938−6945.
(35) Min, J.; Zhang, Z.-G.; Zhang, S.; Li, Y. Conjugated Side-Chain-Isolated D−A Copolymers Based on Benzo[1,2-b:4,5-b′]dithiophene-alt-dithienylbenzotriazole: Synthesis and Photovoltaic Properties. *Chem. Mater.* **2012**, *24*, 3247−3254.
(36) Peng, Q.; Liu, X.; Su, D.; Fu, G.; Xu, J.; Dai, L. Novel Benzo[1,2-b:4,5-b′]dithiophene−Benzothiadiazole Derivatives with Variable Side Chains for High-Performance Solar Cells. *Adv. Mater.* **2011**, *23*, 4554−4558.
(37) Liu, B.; Chen, X.; He, Y.; Li, Y.; Xu, X.; Xiao, L.; Li, L.; Zou, Y. New alkylthienyl substituted benzo[1,2-b:4,5-b′]dithiophene-based polymers for high performance solar cells. *J. Mater. Chem. A* **2013**, *1*, 570−577.
(38) Zhang, M.; Gu, Y.; Guo, X.; Liu, F.; Zhang, S.; Huo, L.; Russell, T. P.; Hou, J. Efficient Polymer Solar Cells Based on Benzothiadiazole and Alkylphenyl Substituted Benzodithiophene with a Power Conversion Efficiency over 8%. *Adv. Mater.* **2013**, *25*, 4944−4949.
(39) Wang, M.; Hu, X.; Liu, P.; Li, W.; Gong, X.; Huang, F.; Cao, Y. Donor−Acceptor Conjugated Polymer Based on Naphtho[1,2-c:5,6-c]bis[1,2,5]thiadiazole for High-Performance Polymer Solar Cells. *J. Am. Chem. Soc.* **2011**, *133*, 9638−9641.
(40) Lee, C.; Giridhar, T.; Choi, J.; Kim, S.; Kim, Y.; Kim, T.; Lee, W.; Cho, H.-H.; Wang, C.; Ade, H.; Kim, B. J. Importance of 2D Conjugated Side Chains of Benzodithiophene-Based Polymers in

https://dx.doi.org/10.1021/acs.macromol.0c01297
Macromolecules 2020, 53, 7740−7748

Controlling Polymer Packing, Interfacial Ordering, and Composition Variations of All-Polymer Solar Cells. *Chem. Mater.* **2017**, *29*, 9407−9415.
(41) Fischer, E.; Larsen, J.; Christensen, J. B.; Fourmigué, M.; Madsen, H. G.; Harrit, N. Synthesis of New Sulfur Heteroaromatics Isoelectronic with Dibenzo[g,p]chrysene by Photocyclization of Thienyl- and Phenyl-Substituted Ethenes. *J. Org. Chem.* **1996**, *61*, 6997−7005.
(42) Dou, C.; Saito, S.; Gao, L.; Matsumoto, N.; Karasawa, T.; Zhang, H.; Fukazawa, A.; Yamaguchi, S. Sequential Electrophilic and Photochemical Cyclizations from Bis(bithienyl)acetylene to a Tetrathienonaphthalene Core. *Org. Lett.* **2013**, *15*, 80−83.
(43) Yamamoto, A.; Ohta, E.; Kishigami, N.; Tsukahara, N.; Tomiyori, Y.; Sato, H.; Matsui, Y.; Kano, Y.; Mizuno, K.; Ikeda, H. Synthesis and basic properties of tetrathieno[2,3-a:3′,2′-c:2″,3″-f:3‴,2‴-h]naphthalene: a new π-conjugated system obtained by photoinduced electrocyclization−dehydrogenation reactions of tetra-(3-thienyl)ethene. *Tetrahedron Lett.* **2013**, *54*, 4049−4053.
(44) Chang, S.-L.; Lu, C.-W.; Lai, Y.-Y.; Hsu, J.-Y.; Cheng, Y.-J. Synthesis and Molecular Properties of Two Isomeric Dialkylated Tetrathienonaphthalenes. *Org. Lett.* **2016**, *18*, 368−371.
(45) Fukazawa, A.; Yamada, H.; Yamaguchi, S. Phosphonium- and Borate-Bridged Zwitterionic Ladder Stilbene and Its Extended Analogues. *Angew. Chem., Int. Ed.* **2008**, *47*, 5582−5585.
(46) Lee, J.; Ko, H.; Song, E.; Kim, H. G.; Cho, K. Naphthodithiophene-Based Conjugated Polymer with Linear, Planar Backbone Conformation and Strong Intermolecular Packing for Efficient Organic Solar Cells. *ACS Appl. Mater. Interfaces* **2015**, *7*, 21159−21169.
(47) Salleo, A. Charge transport in polymeric transistors. *Mater. Today* **2007**, *10*, 38−45.
(48) Kline, R. J.; DeLongchamp, D. M.; Fischer, D. A.; Lin, E. K.; Heeney, M.; McCulloch, I.; Toney, M. F. Significant dependence of morphology and charge carrier mobility on substrate surface chemistry in high performance polythiophene semiconductor films. *Appl. Phys. Lett.* **2007**, *90*, No. 062117.
(49) Piliego, C.; Holcombe, T. W.; Douglas, J. D.; Woo, C. H.; Beaujuge, P. M.; Fréchet, J. M. J. Synthetic Control of Structural Order in N-Alkylthieno[3,4-c]pyrrole-4,6-dione-Based Polymers for Efficient Solar Cells. *J. Am. Chem. Soc.* **2010**, *132*, 7595−7597.

https://dx.doi.org/10.1021/acs.macromol.0c01297
Macromolecules 2020, 53, 7740−7748